Original Article

The molecular basis for p53 inhibition of autophagy in porcine fibroblast cells

Jimin Fei[1#], Anyong Xu[2,3,4#], Wen Zeng[1], Yukun Liu[2,3,5], Deling Jiao[2,3,4], Wanyun Zhu[5], Kaixiang Xu[2,3,4], Honghui Li[2,3,4], Hong-Jiang Wei[2,3,4], Hong-Ye Zhao[2,3,4,5]

[1]The Third Affiliated Hospital of Kunming Medical University, The Tumor Hospital of Yunnan Province, Kunming 650201, China; [2]Key Laboratory of Animal Gene Editing and Animal Cloning in Yunnan Province, Kunming 650201, China; [3]Xenotransplantation Engineering Research Center in Yunnan Province, Kunming 650201, China; [4]State Key Laboratory for Conservation and Utilization of Bio-Resources in Yunnan, Yunnan Agricultural University, Kunming 650201, China; [5]College of Pharmacy and Chemistry, Dali University, Dali 671000, China

Contributions: (I) Conception and design: HY Zhao, HJ Wei; (II) Administrative support: None; (III) Provision of study materials: J Fei, A Xu, Y Liu, D Jiao, W Zeng, H Li; (IV) Collection and assembly of data: A Xu; (V) Data analysis and interpretation: A Xu, HY Zhao, K Xu; (VI): Manuscript writing: All authors; (VII) Final approval of manuscript: All authors.

[#]These authors contributed equally to this work.

Correspondence to: Hong-Ye Zhao. Key Laboratory of Animal Gene Editing and Animal Cloning in Yunnan Province, Kunming 650201, China. Email: hyzhao2000@126.com; Hong-Jiang Wei. Xenotransplantation Engineering Research Center in Yunnan Province, Kunming 650201, China. Email: hongjiangwei@126.com.

Background: Autophagy regulation involves an intricate network that can degrade and recycle cytosolic components in autophagosomes when cells are subject to various stress signals. p53 plays a dual role of induction or inhibition in the regulation of autophagy. Recently, pigs have been considered an excellent large animal model for their many anatomical and physiological similarities to humans. Here, we investigated the relationship between p53 and autophagy, as well as the underling molecular basis, in porcine fibroblast cells (PFCs).

Methods: Autophagy was induced by Earle's balanced salt solution (EBSS) in $p53^{-/-}$ and $p53^{wt}$ PFCs. The autophagy response was assessed by immunoblotting, transmission electron microscopy (TEM) and fluorescent staining. The molecular basis for p53 regulation of autophagy was analyzed by qPCR.

Results: We found that the increased expression of LC3-II and the decreased expression of P62 occurred earlier in $p53^{-/-}$ PFCs than in $p53^{wt}$ PFCs, the relative autophagic flux of $p53^{-/-}$ PFCs was stronger than that of $p53^{wt}$ PFCs in a time-dependent manner. Meanwhile, we observed a visualized increase of autophagosomes in $p53^{-/-}$ PFCs. Moreover, we found greater accumulation of LC3 punctate and acidic vesicular organelle (AVOs) in the cytoplasm of $p53^{-/-}$ PFCs than in that of $p53^{wt}$ PFCs, and these effects were further augmented by Baf A1 treatment. Furthermore, we detected the expression of 6 autophagy signaling pathway-related genes and 14 autophagy-related (*ATG*) genes by qPCR. We found that the expression patterns of the 6 genes had significant differences in both groups of treated PFCs. These results demonstrated that p53 negatively regulated autophagy and involving the downregulation of LMNA gene by p53 via an unknown pathway, which causes the upregulation of the *LC3*, *ULK1*, *ATG4B*, *ATG16L1* and *ATG9A* genes and the downregulation of the *P62* gene.

Conclusions: $p53^{-/-}$ PFCs responded to autophagy earlier than $p53^{wt}$ PFCs, which implied that p53 might inhibit autophagy. The expression patterns of autophagy signaling pathway-related genes and *ATG* genes were most different between $p53^{-/-}$ and $p53^{wt}$ PFCs. Our study will provide a new biological model and contribute to further study of the molecular basis for p53 and autophagy.

Keywords: p53; autophagy; autophagy-related genes (*ATG*); autophagy signaling pathway-related genes; porcine fibroblast cells

Submitted Feb 01, 2019. Accepted for publication May 17, 2019.
doi: 10.21037/tcr.2019.05.22
View this article at: http://dx.doi.org/10.21037/tcr.2019.05.22

Introduction

Autophagy is an evolutionarily conserved homeostatic process that degrades and recycles cytosolic components in autophagosomes (1). When cells are subjected to various stress signals, including nutrient deprivation, autophagy is usually activated (2). This dynamic process is highly controlled by autophagy-related (*ATG*) genes which encode autophagosome formation (3). The core process of autophagy is categorized into five steps: (I) autophagosome formation initiated by the ATG1/ULK1 complex (4); (II) nucleation regulated by the ATG12 conjugation system (5); (III&IV) elongation regulated by the ATG8/LC3 conjugation/deconjugation system and beclin-1/PI3K complex (6); and (V) degradation by the ATG9/ATG9L1 cycling system (7). Additionally, autophagy also regulated by signaling pathways, including p53, PI3K, RAS and JAK-STAT signaling pathways (8). Therefore, autophagy regulation is an intricate network, and the molecular basis for it has not been fully elucidated.

p53, a well-known tumor suppressor, plays an important role in cellular genome stability (9). In response to a myriad of stresses, such as starvation stress, genotoxic stress and other forms of stress, p53 can induce diverse cellular responses, including cell cycle arrest, apoptosis and autophagy (10). Numerous studies have reported that p53 plays a dual role in the regulation of autophagy (11,12).

It has been reported that autophagy is regulated by p53 through signaling pathways in a transcription-dependent or transcription-independent manner. When p53 is activated, autophagy may be induced by inhibiting the mammalian target of rapamycin (mTOR) pathway and activating the AMP-responsive protein kinase (AMPK) pathway (13). Additionally, p53 may also induce autophagy by activating target genes that code for pro-autophagic modulators, including PTEN, DRAM, IGF-BP3, and ARF, and pro-apoptotic Bcl-2 proteins (Bax, PUMA) (10). Strikingly, p53 and TP53-induced glycolysis and apoptosis regulator (TIGAR) may inhibit autophagy directly (14). Several studies indicated that p53 can serve as either an inducer or inhibitor, depending on the cellular context, type of stress and the subcellular localization of p53 (15). However, the mechanism by which p53 regulates autophagy still need to be elucidated.

Previous studies have demonstrated that the deletion or inhibition of p53 induced an autophagy response in human, mouse and nematode cells (16). However, the relationship between autophagy and p53 in PFCs need to be identified. In this study, we investigated the role of p53 in the regulation of autophagy and the molecular difference in the autophagic response in starvation-induced autophagy in PFCs.

Methods

Reagents

Earle's balanced salt solution (EBSS) was purchased from Gibco (St. Louis, MO, USA). Rabbit anti-p62 (Cat# P0067), rabbit anti-LC3B (Cat# L7543) and mouse anti-β-actin (Cat#A5541) were obtained from Sigma-Aldrich (Merck KGaA, Darmstadt, Germany). Bafilomycin A1 (Baf A1) was purchased from Sangon Biotech (Shanghai, China).

Cell lines and cell culture

Wild type p53 ($p53^{wt}$) and p53 knockout ($p53^{-/-}$) PFCs were established and the p53 expression status was confirmed as described in our previous study (17). Cells were cultured in Dulbecco's modified Eagle's medium (DMEM) (Gibco, NY, USA) supplemented with 10% fetal bovine serum (FBS) (Gibco, NY, USA), 100 IU/mL penicillin and 100 IU/mL streptomycin. All cells were incubated in a humidified 5% CO_2 atmosphere at 37 ℃.

Protein extraction and immunoblotting

Protein extraction and immunoblotting were performed according to our previous study (18). Briefly, after treatment, the cells were washed twice with PBS and collected. Then, the cell lysate concentration was determined using a BCA protein assay kit (Beyotime, Shanghai, China). Next, 50 μg of the total protein samples was separated by 12% SDS-PAGE and transferred onto PVDF membranes. The membranes were blocked with 5% BSA (Solarbio, Beijing, China) for 2 h and then incubation with a diluted primary antibody (LC3B: 1:2,000, p62: 1:2,000, β-actin: 1:5,000) overnight at 4 ℃. Subsequently, the membranes were washed and incubated with the appropriate secondary antibodies (R&D, 1:5,000, USA) for 2 h at room temperature. Finally, the membranes were incubated with ECL (Easysee Western Blotting Kit, Transgenes, China) and visualized with an imaging system (Bio-Rad, Hercules, USA).

Transmission electron microscopy (TEM)

Samples used for transmission electron microscopy (TEM) analysis were harvested and washed twice with cold PBS.

Before dehydrated in ethanol, the samples were fixed in 2.5% glutaraldehyde for 30 min at room temperature and incubated overnight at 4 ℃. The samples were washed three times with a 0.1 M phosphoric acid buffer solution and post-fixed with 1% osmium tetroxide for 2–3 h at 4 ℃. Then, the samples were treated with a mixed solution of acetone and embedding solution and embedded in Spurr's resin for the preparation of ultrathin sections. After staining with 3% uranyl acetate and lead citrate, ultrathin sections were examined using a transmission electron microscope (JEM 1011, JEOL, Japan).

Immunofluorescence

The $p53^{wt}$ and $p53^{-/-}$ PFCs (5×10^4 cells/well) were seeded on 6-chamber culture slides and pretreated with Baf A1 (100 nM) for 2 h, followed by treated with EBSS for 2 h. Then, the cells were fixed with 4% paraformaldehyde for 10 min and permeabilized with PBS containing 5% BSA and 0.3% Triton X-100 for 30 min. After that, the cells were incubated with anti-LC3B antibody (1:200 diluted in 1.5% BSA) at 4 ℃ overnight. Cells were then incubated for 1 h with 1:400 secondary FITC-conjugated antibody, followed by incubation with DAPI for nuclear staining. Images were captured with a confocal fluorescence microscope (OLYMPUS FV 1000, Tokyo, Japan).

Acridine orange (AO) staining

To further detect the acidic vesicular organelles (AVOs), vital staining of PFCs with acridine orange (AO) (Sigma-Aldrich, St. Louis, MO, USA) was performed. Briefly, after treatment as described above, $p53^{wt}$ and $p53^{-/-}$ PFCs were stained with AO (5 μg/mL) for 15 min, washed with PBS and then visualized with fluorescence microscope (OLYMPUS IX71, Tokyo, Japan).

Quantitative real-time polymerase chain reactive (q-PCR) assay

$p53^{wt}$ and $p53^{-/-}$ PFCs were treated with EBSS for 2 h. Total RNA was extracted by Trizol (Invitrogen, Carlsbad, CA, USA). cDNA was synthesized from the total RNA using a Prime-Script RT reagent kit (TaKaRa, Tokyo, Japan). The obtained cDNA was used as a template for SYBR Green-based q-PCR (CFX-96, Bio-Rad, Hercules, CA, USA). The mRNA expression levels of the *ATG* genes were assessed with quantitative polymerase chain reaction (q-PCR). GAPDH was used for normalization. The primers used are shown in *Table 1*.

Measurement of autophagy flux

Autophagy flux was assessed in $p53^{wt}$ and $p53^{-/-}$ PFCs. A difference in LC3B-II levels in the presence and absence of lysosomal degradation (Baf A1, 100 nM) represents autophagic flux (19). Autophagy flux (AF) was calculated by the following equations according to the method of Gupta *et al.* (20): UT AF = (UT + Baf A1) – (UT – Baf A1), MT AF = (MT + Baf A1) – (MT – Baf A1), and ΔAF = (MT AF) – (UT AF), where UT is untreated and MT is modulator (EBSS)-treated.

Statistical analysis

Comparisons were performed using Student's *t*-test. Quantitative data are expressed as the means ± SD. *P<0.05 and **P<0.01 versus the control were considered significant.

Results

Effect of starvation on autophagy in $p53^{wt}$ and $p53^{-/-}$ porcine fibroblasts cells

Increased expression of LC3-II and decreased expression of P62 are considered autophagosomal markers, but increases in LC3-II can be caused by increased autophagic flux or can be a result of blocking in autophagosome-lysosome fusion or degradation (19). To distinguish between these two possibilities, we performed an autophagy flux assay using the lysosomal ATPase inhibitor, Baf A1, which blocks lysosomal acidification. Immunoblotting results showed the expression of LC3B-II increased in a time-dependent manner in both groups of treated PFCs. This effect was further augmented by BafA1 treatment (*Figure 1A*,*B*,*C*,*D*). The digital results show that the expression of LC3B-II was significantly increased at 4 h in treated p53-wt PFCs, while the expression of LC3B-II was significantly increased at 2 h in $p53^{-/-}$ PFCs (*Figure 1B*,*D*). Moreover, the relative autophagic flux of $p53^{-/-}$ PFCs was stronger than that of $p53^{wt}$ PFCs at 2 h (*Figure 1E*). Meanwhile, we also found the expression of p62 decreased in a time-dependent manner in both groups of treated PFCs (*Figure 1F*,*G*). In addition, TEM results showed accumulation of autophagosomes production in $p53^{-/-}$ PFCs than in $p53^{wt}$ PFCs (*Figure 2*). These results

Table 1 The primers of q-PCR

Gene	Primers sequence (5' to 3')	
	Forward	Reverse
ULK1	F: CTCCCAGAGTGTCCCTCAAATGC	R: TGCTCCTCTTCTTCTACGTCCAAGC
ULK2	F: AGAACAAGCAGAAGCTCCGAAAGC	R: AGAGCCAATGATTGTGGGTAAAGGA
VPS15	F: TGGCAGCCTTGGGCATAACT	R: GAATCGCCTCCTGGTCACTCC
PIK3C3	F: CAAGTGAGAATGGTCCGAATG	R: GTGGAAGAGTTTGCCTGTTTT
BECN1	F: CAATAACTTCAGGCTGGGTCG	R: CGGCAGCTCCTTAGATTTGTCT
P62	F: CTGTGGCTAGTGGTGGTTGGC	R: CTCGTGGTCGCTGAAGTCTGG
ATG4A	F: GAGCCAATCACCGTTTCTCAG	R: CGTCCACCTCCTCATTTCAGT
ATG4B	F: CACCGTCGCCCAGGTTCTCAA	R: GGTCGGAATCTGCGGGAAAGG
ATG10	F: TTCTTCCCTTCTGCTCATCTT	R: CTGTCTTCGCTCAGTAGGTTAA
ATG16L1	F: GAAGGAACTCGCAGAAGCAGC	R: CGCCTCCCAAAGATATTAGTGATAGA
ATG2A	F: TTCTTCCAGGAGCACCTCAGCC	R: CAGCCACCTCGATAGAGCCCAC
ATG2B	F: TGAGTGACGCTATGGAGGAGA	R: CAAGTGGTGAGTGAATGAGGC
ATG9A	F: CAAGAAGTACAGGCCCGGATTGTG	R: CGCAGAGGCAGGAGGGATTTG
ATG9B	F: GCGGCTTTGCCTGTATCCTGC	R: CATCCGACAAGGTCACTTTGCTGTG
mTOR	F: GTCTGCTGATGGGAGAATGGC	R: GTGAGGTAATGAGATGGGTGAAGG
EPG5	F: TTCAGCATCTTCTTGGGTTCA	R: TTCGCTTGACAAACTGCCTAT
FOXO1	F: ACCGCTTTACAAGTGCCTCTGC	R: GCTCAATGAACATGCCATCCAA
LMNA	F: CGAGGTCAAGTGGGTGTAGGAGG	R: GATGGGAAACACGAGGCAAGG
AMBRA1	F: TGTTGCTCGCTCCTTCTTTTCCTGT	R: ACAGGAAAAGAAGGAGCGAGCAACA
DRAM1	F: ATACAGGAACAACACCTCCAGAAAG	R: CCAACCCAAGAACTAGCGACA
GAPDH	F: ATCAAGAAGGTGGTGAAGCAG	R: CAGCATCAAAAGTGGAAGAGTG

demonstrated that starvation induced autophagy in both $p53^{wt}$ and $p53^{-/-}$ PFCs at different time points, and the initiation time of the autophagy response was earlier in $p53^{-/-}$ PFCs than in $p53^{wt}$ PFCs, which implies that p53 knockout induced autophagy without affecting lysosomal degradation in response to starvation.

Effect of starvation on the formation of LC3 punctate and AVOs in $p53^{wt}$ and $p53^{-/-}$ porcine fibroblasts cells

AVOs can be stained by AO dye and emits bright red fluorescence, which are considered as the indicative of autophagy (21). To further ensure that starvation induced autophagy in $p53^{wt}$ and $p53^{-/-}$ PFCs, LC3 punctate, AVOs were monitored and quantified. As shown in *Figure 3A*, the number of LC3 punctate was significantly increased in the presence of EBSS in both group of PFCs. Moreover, the number of LC3 punctate was significantly increased after treatment with EBSS or combination with EBSS and Baf A1for 2 h in $p53^{-/-}$ PFCs, while the number of LC3 punctate has no effect in $p53^{wt}$ PFCs. In addition, the formation of AVOs was significantly increased after treated with EBSS for 2 h in $p53^{-/-}$ cells, while the formation of AVOs was significantly decreased in the presence of Baf A1. Moreover, the formation of AVOs was no change after treatment with EBSS or combination with EBSS and Baf A1 for 2 h (*Figure 3B*). These results further confirmed that p53 knockout induced an increasing autophagy flux without affecting lysosomal degradation in response to starvation, while the autophagy flux of $p53^{wt}$ PFCs had no change.

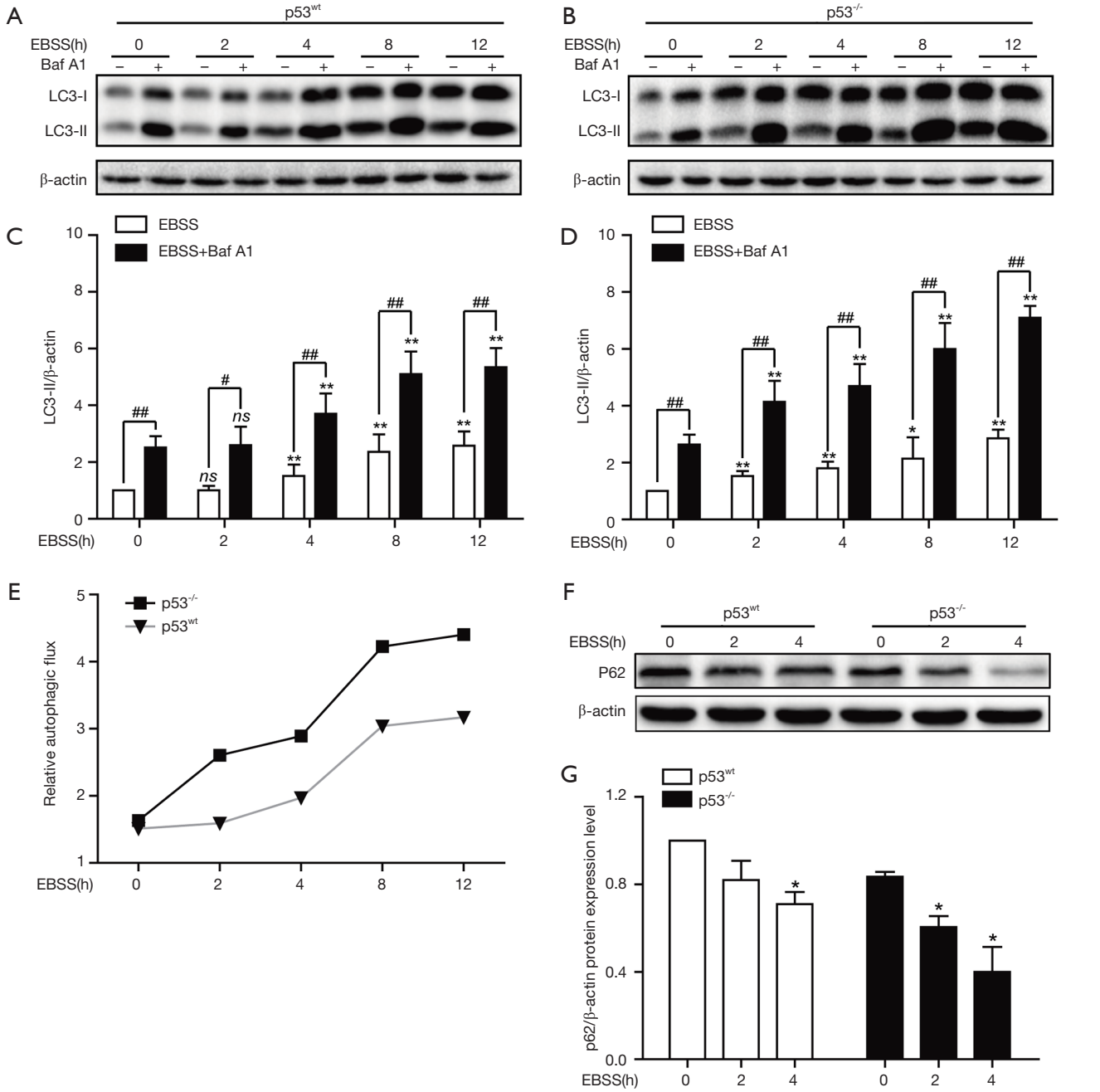

Figure 1 Effect of starvation on autophagy in p53^{wt} and p53$^{-/-}$ PFCs. (A,B) Both cell lines were treated with EBSS for indicated time in the presence or absence of Baf A1 (100 nM). The expression level of the LC3-II protein was analyzed by immunoblotting in p53^{wt} and p53$^{-/-}$ PFCs, β-actin was used as an internal control. (C,D) Quantification of the expression level of the LC3-II protein in p53^{wt} and p53$^{-/-}$ PFCs. All data are expressed as the mean ± SD (n=3). *P<0.05 and **P<0.01 compared to EBSS treated PFCs or combination EBSS with BafA1 treated PFCs at 0 h, $^{\#}$P<0.05 and $^{\#\#}$P<0.01 compared to EBSS treated PFCs at indicated time. (E) Autophagic flux was calculated by subtracting the value of LC3-II in the presence of Baf A1 from that in the absence of Baf A1. (F) The expression level of p62 protein was assessed by immunoblotting after treated with EBSS for indicated time in p53^{wt} and p53$^{-/-}$ PFCs. β-actin was used as an internal control. (G) Quantification of the expression levels of the p62 protein. *P<0.05 and **P<0.01 compared to EBSS treated PFCs at 0 h in both group cells. PFCs, porcine fibroblast cells; EBSS, Earle's balanced salt solution.

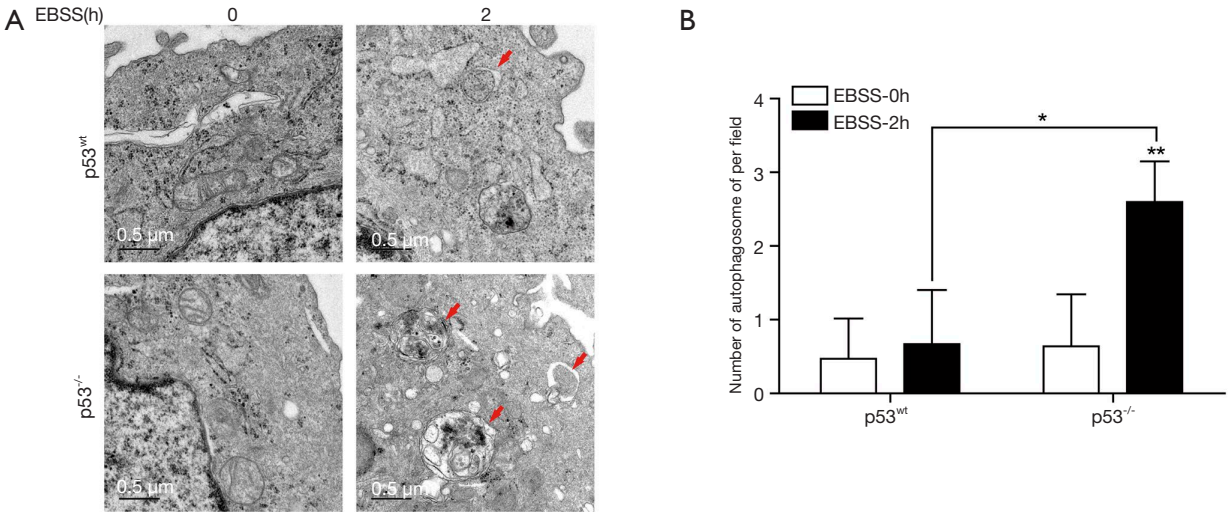

Figure 2 Effect of starvation on the autophagosome accumulation in $p53^{wt}$ and $p53^{-/-}$ PFCs. (A) TEM images of both PFCs after treated with EBSS for 0 and 2 h (magnification, ×40,000). The red arrows refer to autophagosomes. Scale bars =0.5 μm. (B) Quantification of the number of autophagosomes in each section with ~10 cells. All data are expressed as the mean ± SD. *P<0.05 compared to EBSS treated $p53^{wt}$ PFCs at 2 h, **P<0.01 compared to EBSS treated $p53^{-/-}$ PFCs at 0 h. PFCs, porcine fibroblast cells; EBSS, Earle's balanced salt solution.

Effect of starvation on the mRNA expression level of autophagy signaling pathway-related genes in $p53^{wt}$ and $p53^{-/-}$ porcine fibroblasts cells

The genes upstream of autophagy, including *FOXO1*, *mTOR*, *EPG5*, *LMNA*, *AMBRA1* and *DRAM1*, induce autophagy through signaling pathways (22-24). We found that the mRNA expression levels of the autophagy signaling pathway-related genes *EPG5*, *AMBRA1* and *DRAM1* were significantly increased in both types of cells; the expression of the LMNA gene was down-regulated significantly in $p53^{-/-}$ PFCs, but was unchanged in $p53^{wt}$ PFCs. In addition, the expression of the *FOXO1* gene was up-regulated significantly in $p53^{wt}$ PFCs, but unchanged in $p53^{-/-}$ PFCs (*Figure 4*). These results demonstrated that the partial autophagy signaling pathway response might be different in the two types of PFCs.

Effect of starvation on the mRNA expression level of autophagy-related genes in $p53^{wt}$ and $p53^{-/-}$ porcine fibroblasts cells

Autophagy is a classic and highly conserved catabolic process, that includes initiation, nucleation, elongation and degradation cycling, which are controlled by autophagy-related genes. The initiation of autophagy begins with activation of the *ULK1* complex, including *ULK1*, *ULK2*, *ATG13*, *FIP200* (also known as *RB1CC1*) and *ATG101*, which activates nucleation-related genes. A class III PI3K complex (*VPS15*, *PIK3C3* and *BECN1*), *ATG4A*, *ATG4B*, *ATG10* and *ATG16L1* are conducive to elongation, and *ATG2A*, *ATG2B*, *ATG9A* and *ATG9B* are the degradation cycling-related genes (25). To determine the autophagy-related gene response of both types of treated PFCs, we detected the mRNA expression levels of the autophagy-related genes described above by qPCR. We found the following: the mRNA expression levels of the *ULK1*, *ULK2*, *VPS15*, *PIK3C3*, *BECN1*, *ATG4A*, *ATG4B*, *ATG16L1*, *ATG9A*, *ATG2A* and *ATG2B* genes were significantly increased, and *p62* was significantly decreased after treated EBSS at 2h than treated with EBSS at 0 h in $p53^{-/-}$ PFCs (*Figure 5*). The mRNA expression levels of the *ULK2*, *VPS15*, *PIK3C3*, *BECN1*, *ATG4A*, *ATG2A*, *ATG2B* and *ATG10* genes were significantly increased at 2 h, whereas the mRNA expression levels of the ATG16L1 and *p62* genes were significantly decreased after EBSS treated at 2 h than EBSS treated at 0h in $p53^{wt}$ PFCs (*Figure 5*). Interestingly, we found that the expression of the *ULK1*, *ATG4B* and *ATG9A* genes was up-regulated in $p53^{-/-}$ PFCs, while these genes had no change in $p53^{wt}$ PFCs. Additionally, the expression of *ATG16L1* was up-regulated in $p53^{-/-}$ PFCs but down-regulated in $p53^{wt}$ PFCs. These results demonstrated that the autophagy-related gene response in the process of autophagosome formation was distinctly different in both

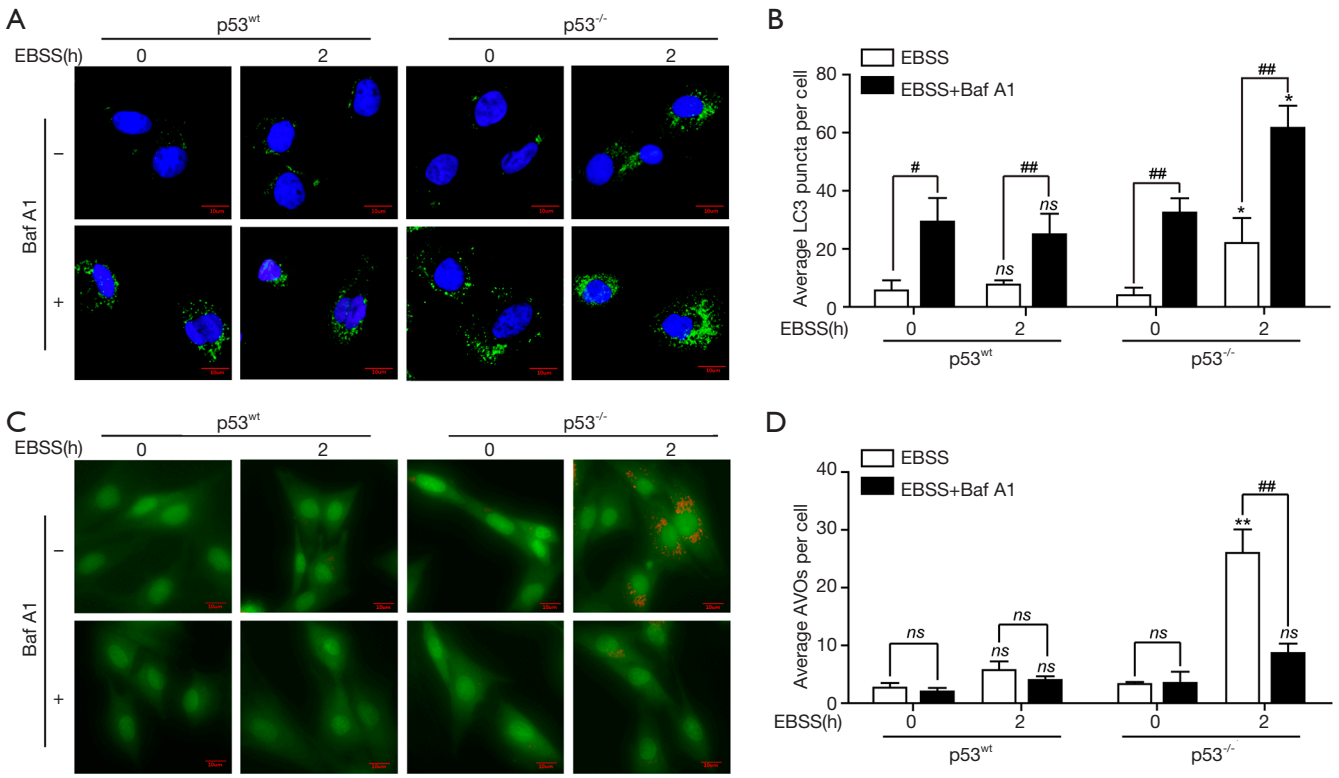

Figure 3 Effect of starvation on the formation of LC3 punctate and AVOs in p53^{wt} and p53$^{-/-}$ PFCs. Both cell lines were treated with EBSS for 0 and 2 h in the presence or absence of Baf A1 (100 nM), cell were stained for LC3 or acridine orange (AO) and visualized with fluorescence microscopy. (A) Representative images of LC3 punctate in both treated PFCs. Cells were stained with antibodies against LC3 (green), the nuclei are stained blue with DAPI. Scale bars =10 μm. (B) The quantification of average of LC3 punctate per cell in both treated PFCs. *P<0.05 and **P<0.01 compared to EBSS treated PFCs or combination EBSS with BafA1 treated PFCs at 0 h, $^{\#}$P<0.05 and $^{\#\#}$P<0.01 compared to EBSS treated PFCs at indicated time. (C) Representative images of acidic vesicular organelles (AVOs) in both treated cell lines. Scale bars =10 μm. (D) The quantification of average of AVOs per cell in both of cell types. *P<0.05 and **P<0.01 compared to EBSS treated PFCs or combination EBSS with BafA1 treated PFCs at 0 h, $^{\#}$P<0.05 and $^{\#\#}$P<0.01 compared to EBSS treated PFCs at indicated time. PFCs, porcine fibroblast cells; EBSS, Earle's balanced salt solution.

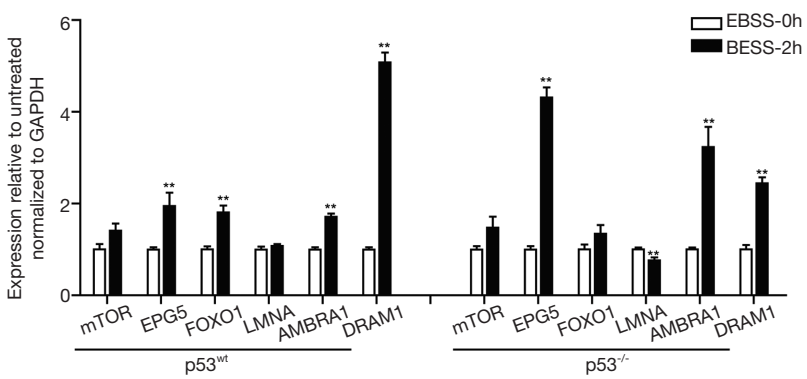

Figure 4 Effect of starvation on the mRNA expression levels of autophagy signaling pathway-related genes in p53^{wt} and p53$^{-/-}$ porcine fibroblast cells. Both types of cells were treated with EBSS for 0 h and 2 h. (A) mRNA expression levels of the autophagy signaling pathway-related genes *mTOR*, *EPG5*, *FOXO1*, *LMNA*, *AMBRA1* and *DRAM1* in both treated cell lines. All data are expressed as the mean ± SD (n=3). *P<0.05 and **P<0.01 compared to the EBSS treated at 0 h in both PFCs. PFCs, porcine fibroblast cells; EBSS, Earle's balanced salt solution.

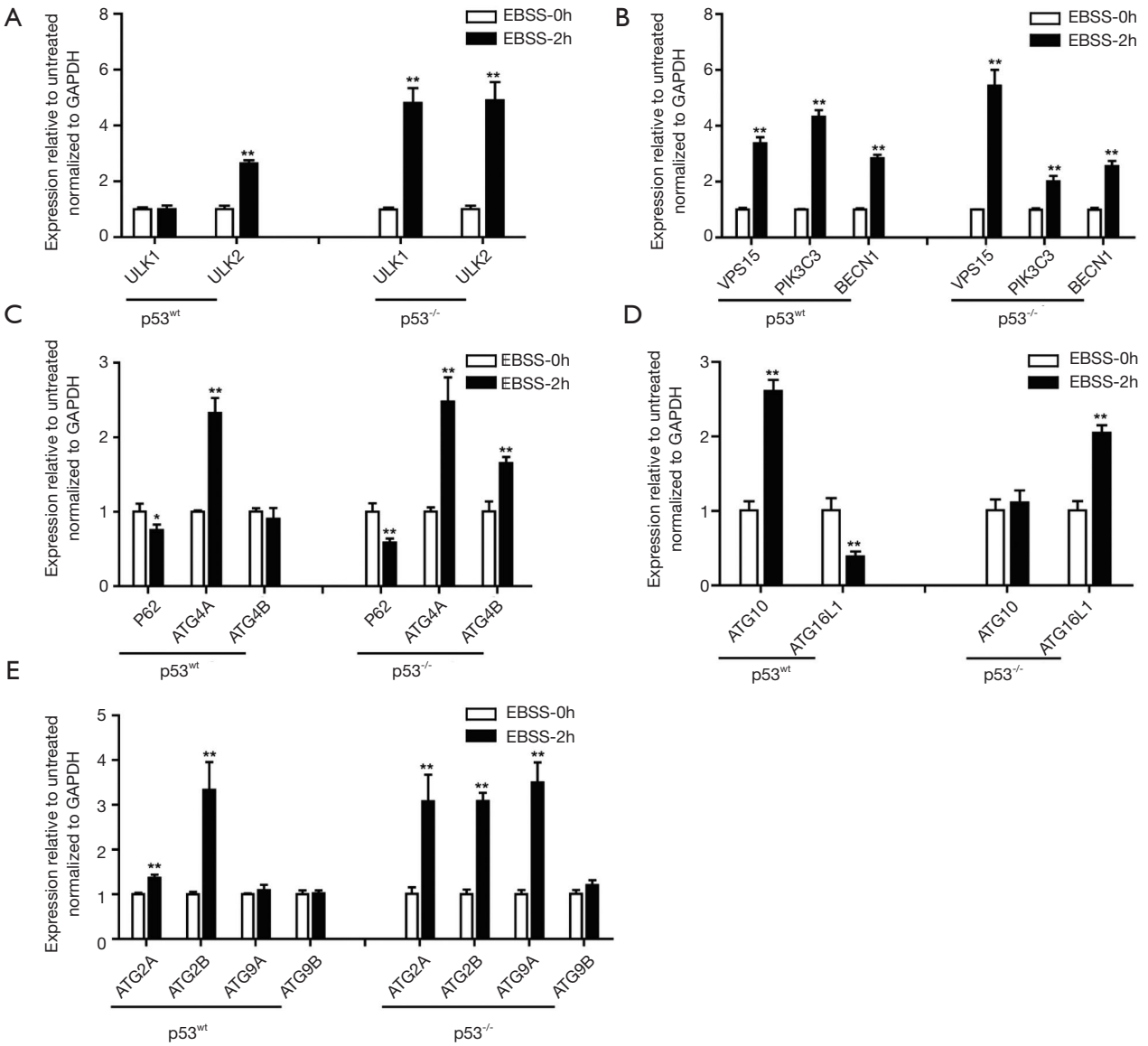

Figure 5 Effect of starvation on the mRNA expression levels of *ATG* genes in $p53^{wt}$ and $p53^{-/-}$ PFCs. Both types of cells were treated as described above. (A) mRNA expression levels of the autophagosome initiation-related genes *ULK1* and *ULK2* in both types of treated cells. (B) mRNA expression levels of the nucleation-related genes *VPS15*, *PIK3C3* and *BECN1* in both types of treated cells. (C) mRNA expression levels of the elongation-related genes *ATG4A*, *ATG4B*, and *p62* in both types of treated cells. (D) mRNA expression levels of the elongation-related genes *ATG10* and *ATG16L1* in both types of treated cells. (E) mRNA expression levels of the degradation cycling-related genes *ATG2A*, *ATG2B*, *ATG9A* and *ATG9B* in both types of treated cells. All data are expressed as the mean ± SD (n=3). *P<0.05 and **P<0.01 compared to the EBSS treated at 0 h in both PFCs. PFCs, porcine fibroblast cells; EBSS, Earle's balanced salt solution.

types of treated PFCs.

Discussion

The relationship between p53 and autophagy regulation is an intricate one. Some previous studies have shown that p53 positively regulates autophagy (26), but downregulation of p53 induces autophagy in human trophoblast differentiation (27). Tasdemir *et al.* indicated that pharmacological inhibition and knockdown or knockout of p53 can induce autophagy in mouse and nematode cells (28). Our results were consistent with this finding. In this study, we found starvation-induced

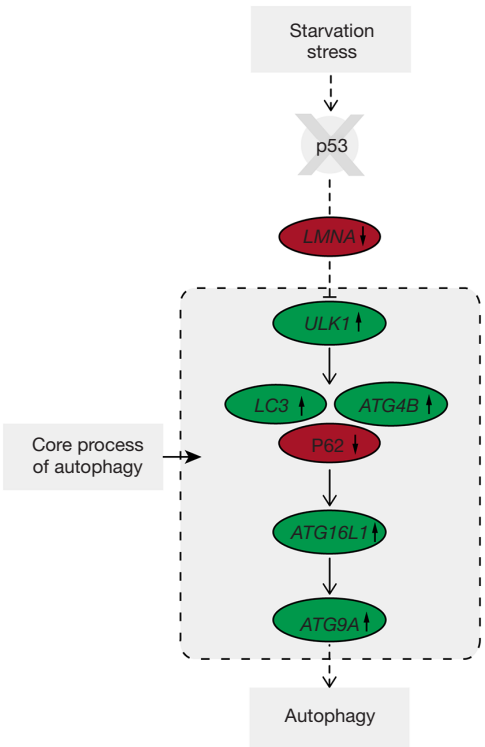

Figure 6 Schematic pathway showing the negative regulation of autophagy by p53 knockout in PFCs during starvation stress. In this model, autophagy was induced involving the downregulation of *LMNA* by p53 via an unknown pathway, which causes the upregulation of the *LC3*, *ULK1*, *ATG4B*, *ATG16L1* and *ATG9A* genes and the downregulation of the *p62* gene. The green background indicates the upregulated proteins or genes and red background indicates the downregulated proteins or genes. PFCs, porcine fibroblast cells.

autophagy in $p53^{wt}$ and $p53^{-/-}$ PFCs (*Figures 1-3*), implying that p53 negatively regulates autophagy in response to starvation. Interestingly, we found that the initiation time of the autophagy response was earlier in $p53^{-/-}$ PFCs than in $p53^{wt}$ PFCs (*Figure 1*). It has been reported that autophagy is regulated by Ras signaling or JAK-STAT signaling under nutrient depletion (8). The p53-mediated autophagy may be related to cell type, stress-specific or activation of other p53 signaling pathway, which need further study.

The *LMNA* gene, which encodes lamin A and C (lamin A/C), could inhibit autophagy by activating mTOR in a mouse model (22). Of the autophagy signaling pathway-related genes, *LMNA* gene levels were lower in treated $p53^{-/-}$ PFCs than in treated $p53^{wt}$ PFCs, while *FOXO1* gene levels were higher in treated $p53^{wt}$ PFCs than in treated $p53^{-/-}$ PFCs (*Figure 4*). These findings suggested that p53 may negatively regulate autophagy in a transcription-independent manner through targeting the LMNA/AKT/mTOR signaling pathway and positively regulate autophagy by targeting the PI3K/AKT/FOXO1 signaling pathway. Consistently, some studies also reported that the LMNA/AKT/mTOR and PI3K/AKT/FOXO1 signaling pathways may regulate autophagy in MCF-7 and MDA-MB-231 breast cancer cells and in other cells (18,29). Therefore, the role of p53 in controlling autophagy in PFCs requires further study.

The molecular basis of autophagy has been studied extensively in the setting of starvation stress, in which ATG proteins induction of autophagosome formation is considered basic research. ULK1 is a serine/threonine kinase that plays a role in autophagy by recruiting downstream ATG proteins (30). The *ATG4B*, *ATG9* and *ATG16L1* genes are essential for autophagosome elongation, maturation and degradation (31). In this study, we found that the levels of the *ULK1*, *ATG4B* and *ATG9A* genes were higher in treated $p53^{-/-}$ PFCs than in treated $p53^{wt}$ PFCs. In addition, the *ATG16L1* gene was downregulated in treated $p53^{wt}$ PFCs but upregulated in treated $p53^{-/-}$ PFCs (*Figure 5*). It has been indicated that the dephosphorylation of ULK1 at Ser637 occurs in a p53-dependent manner in p53-null mouse embryonic fibroblasts (32). These findings suggest that p53 may negatively regulate autophagy in a transcription-independent manner through targeting the *ULK1*, *ATG4B*, *ATG16L1* and *ATG9A* genes. However, the specific mechanism involved in targeting the *ULK1*, *ATG4B*, *ATG16L1* and *ATG9A* genes requires further study.

Conclusions

In conclusion, our findings indicated that p53 negatively regulated autophagy under starvation conditions in PFCs, the autophagic flux of $p53^{-/-}$ PFCs increased without affecting lysosomal degradation in response to starvation in early phase. Furthermore, we hypothesized that targeting *ATG* genes and signaling pathways via p53 knockout would induce a response to starvation. A schematic representation of the proposed mechanism of autophagy regulation by p53 knockout in PFCs proposed in the present study is shown in *Figure 6*. These findings will provide a new biological model and support further study of the molecular mechanism of p53 in controlling autophagy in response to starvation.

Acknowledgments

Funding: This work was supported by the National Natural Science Foundation of China (No. 81872452, and 31760671) and Yunnan Province Science and Technology Department Expert Workstation (No. 2017IC010).

Footnote

Conflicts of Interest: All authors have completed the ICMJE uniform disclosure form (available at http://dx.doi.org/10.21037/tcr.2019.05.22). The authors have no conflicts of interest to declare.

Ethical Statement: The authors are accountable for all aspects of the work in ensuring that questions related to the accuracy or integrity of any part of the work are appropriately investigated and resolved. All experiments in our study were approved by the Institutional Animal Care and Use Committee of Yunnan Agricultural University (permission code: YAUACUC01; date of publication: 10 July 2013).

References

1. Wang S, Xia P, Rehm M, et al. Autophagy and cell reprogramming. Cell Mol Life Sci 2015;72:1699-713.
2. Gatica D, Lahiri V, Klionsky DJ. Cargo recognition and degradation by selective autophagy. Nat Cell Biol 2018;20:233-42.
3. Galluzzi L, Baehrecke EH, Ballabio A, et al. Molecular definitions of autophagy and related processes. EMBO J 2017;36:1811-36.
4. Mizushima N. The role of the Atg1/ULK1 complex in autophagy regulation. Curr Opin Cell Biol 2010;22:132-9.
5. Funderburk SF, Wang QJ, Yue Z. Beclin 1-VPS34 complex – At the Crossroads of Autophagy and Beyond. Trends Cell Biol 2010;20:355-62.
6. Xu DW, Zhang GQ, Wang ZW, et al. Autophagy in tumorigenesis and cancer treatment. Asian Pac J Cancer Prev 2015;16:2167-75.
7. Yamamoto H, Kakuta S, Watanabe TM, et al. Atg9 vesicles are an important membrane source during early steps of autophagosome formation. J Cell Biol 2012;198:219-33.
8. Levy JMM, Towers CG, Thorburn A. Targeting autophagy in cancer. Nat Rev Cancer 2017;17:528.
9. Kastenhuber ER, Lowe SW. Putting p53 in Context. Cell 2017;170:1062-78.
10. Sui X, Han W, Pan H. p53-induced autophagy and senescence. Oncotarget 2015;6:11723-4.
11. Lu Z, Chen C, Wu Z, et al. A Dual Role of P53 in Regulating Colistin-Induced Autophagy in PC-12 Cells. Front Pharmacol 2017;8:768.
12. Tasdemir E, Maiuri MC, Morselli E, et al. A dual role of p53 in the control of autophagy. Autophagy 2008;4:810-4.
13. Feng Z, Zhang H, Levine AJ, et al. The coordinate regulation of the p53 and mTOR pathways in cells. Proc Natl Acad Sci U S A 2005;102:8204-9.
14. Denisenko TV, Pivnyuk AD, Zhivotovsky B. p53-Autophagy-Metastasis Link. Cancers (Basel) 2018;10:148.
15. Levine B, Abrams J. p53: The Janus of autophagy? Nature Cell Biology 2008;10:637-9.
16. Tang J, Di J, Cao H, et al. p53-mediated autophagic regulation: A prospective strategy for cancer therapy. Cancer Lett 2015;363:101-7.
17. Shen Y, Xu K, Yuan Z, et al. Efficient generation of P53 biallelic knockoutDiannanminiature pigs via TALENs and somatic cell nuclear transfer. J Transl Med 2017;15:224.
18. Zhu W, Qu H, Xu K, et al. Differences in the starvation-induced autophagy response in MDA-MB-231 and MCF-7 breast cancer cells. Anim Cells Syst (Seoul) 2017;21:190-8.
19. Klionsky DJ, Abdalla FC, Abeliovich H, et al. Guidelines for the use and interpretation of assays for monitoring autophagy. Autophagy 2012;8:445-544.
20. Gupta NA, Kolachala VL, Jiang R, et al. Mitigation of autophagy ameliorates hepatocellular damage following ischemia-reperfusion injury in murine steatotic liver. Am J Physiol Gastrointest Liver Physiol 2014;307:G1088-99.
21. Paglin S, Hollister T, Delohery T, et al. A novel response of cancer cells to radiation involves autophagy and formation of acidic vesicles. Cancer Res 2001;61:439-44.
22. Choi JC, Worman HJ. Reactivation of autophagy ameliorates LMNA cardiomyopathy. Autophagy 2013;9:110-1.
23. Li X, Wu C, Chen N, et al. PI3K/Akt/mTOR signaling

pathway and targeted therapy for glioblastoma. Oncotarget 2016;7:33440-50.
24. Miki Y, Tanji K, Mori F, et al. Autophagy mediators (FOXO1, SESN3 and TSC2) in Lewy body disease and aging. Neurosci Lett 2018;684:35-41.
25. Dikic I, Elazar Z. Mechanism and medical implications of mammalian autophagy. Nat Rev Mol Cell Biol 2018;19:349-64.
26. White E. Autophagy and p53. Cold Spring Harb Perspect Med 2016;6:a026120.
27. Gauster M, Maninger S, Siwetz M, et al. Downregulation of p53 drives autophagy during human trophoblast differentiation. Cell Mol Life Sci 2018;75:1839-55.
28. Tasdemir E, Maiuri MC, Galluzzi L, et al. Regulation of autophagy by cytoplasmic p53. Nat Cell Biol 2008;10:676-87.
29. Alers S, Löffler AS, Wesselborg S, et al. Role of AMPK-mTOR-Ulk1/2 in the regulation of autophagy: cross talk, shortcuts, and feedbacks. Mol Cell Biol 2012;32:2-11.
30. Park JM, Seo M, Jung CH, et al. ULK1 phosphorylates Ser30 of BECN1 in association with ATG14 to stimulate autophagy induction. Autophagy 2018;14:584-97.
31. Soto-Burgos J, Zhuang X, Jiang L, et al. Dynamics of autophagosome formation. Plant Physiol 2018;176:219-29.
32. Torii S, Yoshida T, Arakawa S, et al. Identification of PPM1D as an essential Ulk1 phosphatase for genotoxic stress-induced autophagy. EMBO Rep 2016;17:1552-64.

Cite this article as: Fei J, Xu A, Zeng W, Liu Y, Jiao D, Zhu W, Xu K, Li H, Wei HJ, Zhao HY. The molecular basis for p53 inhibition of autophagy in porcine fibroblast cells. Transl Cancer Res 2019;8(3):876-886. doi: 10.21037/tcr.2019.05.22

